Up-regulation of a cellular protein at the translational level by a retrovirus

Fayth K. Yoshimura*†‡, Xixia Luo*, Xiaoqing Zhao*, Herve C. Gerard*, and Alan P. Hudson*

*Department of Immunology and Microbiology and the †Karmanos Cancer Institute, Wayne State University, Detroit, MI 48201

Edited by Stephen P. Goff, Columbia University College of Physicians and Surgeons, New York, NY, and approved February 28, 2008 (received for review November 5, 2007)

Mink cell focus-forming (MCF) murine leukemia viruses (MLVs) are the etiologic agent of thymic lymphoma in mice. We have observed previously that superinfection by MCF13 MLV of certain cell types, such as preleukemic thymic lymphocytes and cultured mink epithelial cells, results in the accumulation of the viral envelope precursor polyprotein, leading to the induction of endoplasmic reticulum (ER) stress. In this study, we demonstrate that the induction of ER stress by MCF13 MLV infection results in an increase in the phosphorylation of the α-subunit of eukaryotic initiation factor 2. In cells in which this occurs, we have detected an up-regulation of the cellular inhibitor of apoptosis protein 1 (c-IAP1). The results of real-time RT-PCR quantification of message levels and protein turnover assays indicate that up-regulation of c-IAP1 occurs at the translational level. Elevation of c-IAP1 levels at a posttranscriptional step was detectable in MCF13 MLV-induced thymic lymphomas and chronically infected mink epithelial cells. The ability of a simple retrovirus to regulate cellular gene expression at the translational level may be an important mechanism that contributes to pathogenesis.

cellular inhibitor of apoptosis protein 1 | endoplasmic reticulum stress | murine leukemia virus

Viruses have evolved a variety of mechanisms to interfere with the host cell translational machinery to promote their own replication. Simple retroviruses, which do not encode regulatory and accessory proteins, are able to regulate cellular proteins at the transcriptional level by a mechanism referred to as insertional mutagenesis as an important step in tumor development (1). Whether this type of retrovirus can also regulate cellular protein expression by other mechanisms is not known. To identify early events that contribute to tumorigenesis, we have used an animal model that involves the induction of thymic lymphoma by mink cell focus-forming (MCF) murine leukemia viruses (MLVs) (2). MCF MLVs are slow transforming gammaretroviruses that lack an oncogene and possess a simple genome (3). We have observed that an early event in tumorigenesis by MCF13 MLV, a strain of MCF MLVs, is the induction of cytopathic effects via apoptosis in thymic lymphocytes (4). To facilitate further studies of the cytopathic effect of this retrovirus, we established an *in vitro* system in which CCL64 mink lung epithelial cells also undergo apoptosis by virus infection (5). The ability to induce cytopathic effects in different cell types has also been demonstrated for other slow-transforming retroviruses, and this ability strongly correlates with viral pathogenesis (6–9). By what means a cell that is infected by a cytopathic retrovirus can be rescued from apoptosis and whether this has a role in tumorigenesis are not known.

We have demonstrated that the cytopathic effect of MCF13 MLV requires virus superinfection, a result of which is the accumulation of high levels of the viral envelope (Env) precursor polyprotein (10). In addition, inefficient processing of the Env polyprotein in the endoplasmic reticulum (ER) contributes to its accumulation in MCF13 MLV-infected cells (46). The accumulation of high levels of secretory and cell-surface proteins in the ER can induce a cellular response referred to as ER stress (11). ER stress responses, which include the up-regulation of ER-localized chaperone proteins, such as the glucose-regulated protein of 78 kDa/Ig heavy-chain binding protein (GRP78/BiP), or activation of ER protein kinases, such as the PKR-like ER kinase (PERK), result in either cell survival or apoptosis. The mechanisms that determine whether a cell survives or undergoes apoptosis in response to ER stress are not well understood. We have demonstrated that ER stress is induced in MCF13 MLV-infected cells, including preleukemic thymic lymphocytes in mice and mink epithelial cells in culture, in which accumulation of the Env precursor polyprotein occurs (10, 12). In our identification of some of the downstream events related to the induction of ER stress and apoptosis by MCF13 MLV, we have determined that this retrovirus uses a mechanism that involves translational control to up-regulate the cellular inhibitor of apoptosis protein 1 (c-IAP1).

Results

Increase in Phosphorylation of the α-Subunit of the Eukaryotic Initiation Factor 2 (eIF2α) by MCF13 MLV Infection of Mink Epithelial Cells. It has been shown that PERK activation by ER stress results in an increase in the phosphorylated form of eIF2α (eIF2α-P) (13, 14). High levels of eIF2α-P can result in the inhibition of cap-dependent protein synthesis but an increase in cap-independent translation of certain mRNAs that contain internal ribosome entry sites (IRES) in their 5′ UTR (15). To examine whether the induction of ER stress by MCF13 MLV infection also results in the up-regulation of eIF2α phosphorylation, we performed *in vitro* studies using mink epithelial cells. In a time-course study, we infected mink cells with MCF13 MLV at a multiplicity of infection (MOI) of 1 and analyzed cellular extracts at different times after virus infection. Immunoblotting revealed that eIF2α-P increased in virus-infected cells starting at 4 days postinfection (p.i.) when it was ≈3-fold greater than that in mock-infected cells (Fig. 1*A*). Comparisons of protein band intensities for all immunoblots were determined by densitometric scanning and analysis with a Kodak EDAS 120 scanner and software. eIF2α-P levels in MCF13 MLV-infected cells continued to increase over time so that they were 5- to 6-fold greater than that in mock-infected cells from days 6 to 11 p.i. We furthermore observed that the increase in eIF2α-P was not caused by an increase in the total eIF2α level (Fig. 1*B*) and therefore represented an increase in phosphorylation of existing levels of this factor. This finding is consistent with what has been observed for eIF2α as a result of cellular stress induced by other means (14). The induction of ER stress in MCF13 MLV-infected cells was verified by a detectable increase in two ER stress-associated markers, GRP78 and the C/EBP homologous protein (CHOP) (10) (Fig. 2 *A* and *B*).

Author contributions: X.L. and X.Z. contributed equally to this work; F.K.Y. designed research; X.L., X.Z., and H.C.G. performed research; X.L., X.Z., H.C.G., and A.P.H. analyzed data; and F.K.Y. wrote the paper.

The authors declare no conflict of interest.

This article is a PNAS Direct Submission.

‡To whom correspondence should be addressed. E-mail: fyoshi@med.wayne.edu.

MICROBIOLOGY

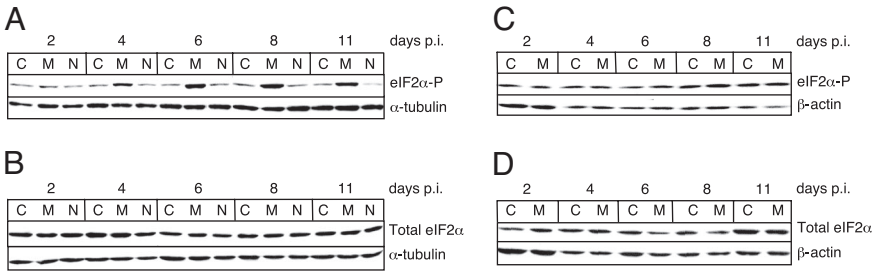

Fig. 1. Up-regulation of eIF2α phosphorylation in cells that undergo ER stress by MLV infection. (*A*) Immunoblot of eIF2α-P in mink epithelial cells either mock-infected as control (C) or infected with either MCF13 MLV (M) or NZB-9 MLV (N) that was detectable with an anti-eIF2α-P that specifically recognizes phosphorylation at Ser-51 (ab4837; Abcam). (*B*) Total eIF2α in the same cells as described in *A* that was detectable with anti-total eIF2α (ab5369; Abcam). (*C*) eIF2α-P in *M. dunni* fibroblasts either mock-infected (C) or infected with MCF13 MLV (M). (*D*) Total eIF2α in the same cells as in *C*. All virus infections were performed at a MOI of 1. Cellular protein was analyzed at different days p.i. α-Tubulin or β-actin was detected as a loading control.

Thus, an increase in eIF2α phosphorylation correlates with MCF13 MLV-induced ER stress.

To demonstrate further that an increase in phosphorylation of eIF2α in mink cells depends on the induction of ER stress by MCF13 MLV, we compared different conditions of MLV infection of different cell types when ER stress is not induced. These conditions included mink cells infected with the xenotropic NZB-9 MLV and *Mus dunni* fibroblasts infected with MCF13 MLV, as we have shown (10). When infection of each cell type with the respective MLV was performed at the same MOI as for MCF13 MLV infection of mink cells, no increase in the level of eIF2α-P was detectable (Fig. 1 *A* and *C*). There was also no effect on the level of total eIF2α under these conditions (Fig. 1 *B* and *D*). The absence of the induction of ER stress in these virus-infected cells was verified by a lack of GRP78 and CHOP up-regulation (Fig. 2). These results further support our conclusion that the up-regulation of eIF2α phosphorylation depends on the ability of an MLV to induce ER stress.

Up-Regulation of c-IAP1 in MCF13 MLV-Infected Cells. Other investigators (15–17) have demonstrated that elevated eIF2α-P levels promote the translation of cellular mRNAs that contain an IRES in the 5′ UTR. Several of the cellular mRNAs that contain IRES sequences encode proteins that possess antiapoptotic activity (15, 18–20). Upon examining these antiapoptotic proteins in mink cells infected with MCF13 MLV at MOI of 20, we observed an up-regulation of c-IAP1 beginning at day 2 p.i. (Fig. 3*A*). c-IAP1 protein level continued to increase over time and was ≈10-fold greater than that in mock-infected cells at day 11 p.i., the last time point examined in this study. As a control, mink cells were treated with tunicamycin and thapsigargin, which also induce c-IAP1 up-regulation as a result of ER stress (20) (Fig. 3*A*, lanes 14 and 15). A band migrating more slowly than c-IAP1 was a result of nonspecific antibody binding. No increase in the level of other antiapoptotic proteins that are potentially translated via IRES sequences, such as Bcl-2, Bcl-X_L, or XIAP, was detectable (data not shown). c-IAP1 up-regulation by virus infection was also detectable at a lower MOI of 1, although with slightly slower kinetics and a lower level of maximum increase of ≈3.5-fold at day 8 p.i. compared with a MOI of 20 (Fig. 3*B*). No increase in c-IAP1 was detectable in either mink cells that were infected with NZB-9 MLV (Fig. 3*B*, lanes 3, 6, 9, 12, and 15) or *M. dunni* cells infected with MCF13 MLV (Fig. 3*C*), conditions under which ER stress is not induced (Fig. 2) (10), and as a result, eIF2α-P was not up-regulated (Fig. 1). Thus, there is a strong correlation between the ability of an MLV to induce elevated eIF2α-P levels via ER stress and the up-regulation of the c-IAP1 protein. Notably, the up-regulation of c-IAP1 in MCF13 MLV-infected mink cells coincided with the time of onset of ER stress, as indicated by the up-regulation of eIF2α-P, GRP78, and CHOP at a MOI of 1 (Figs. 1*A* and 2 *A* and *B*).

Posttranscriptional Up-Regulation of c-IAP1. Because MLVs are known to up-regulate cellular proteins via insertional mutagenesis that results in the augmentation of cellular gene transcription (1), we examined c-IAP1 transcript levels to determine whether this mechanism could account for the increase in protein that was detectable. To quantify c-IAP1 mRNA, we isolated cellular RNA from mock- and virus-infected mink cells at two different times p.i. when an increase in c-IAP1 protein was detectable, i.e., at days 5 and 11 p.i. (Fig. 3), and performed real-time quantitative RT-PCR (qRT-PCR) analysis (Fig. 4*A*). No significant difference in c-IAP1 mRNA levels between mock- and virus-infected cells at either time point was detectable as indicated by *P* values that were determined by Student's *t* test and that were 0.2 for day 5 p.i. and 0.9 for day 11 p.i. These results indicated that the up-regulation of c-IAP1 protein is occurring at a posttranscriptional step.

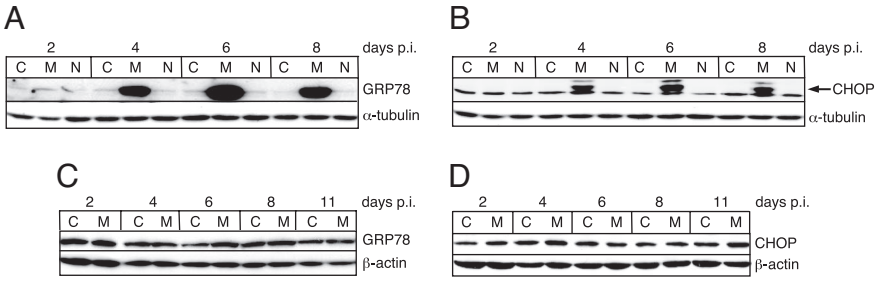

Fig. 2. ER stress-induced proteins in virus-infected cells. (*A*) Immunoblots for GRP78 in mink epithelial cells either mock-infected as control (C) or infected with either MCF13 (M) or NZB-9 (N) MLV. (*B*) CHOP for the same protein samples shown in *A*. (*C*) GRP78 in *M. dunni* fibroblasts that were infected with MCF13 MLV (M) or mock-infected (C). (*D*) CHOP for the same protein samples shown in *C*. Minor bands seen in *B* are a result of nonspecific antibody binding. Virus infections were performed at a MOI of 1. Cellular protein was analyzed at different days p.i. α-Tubulin or β-actin was detected as a control for loading.

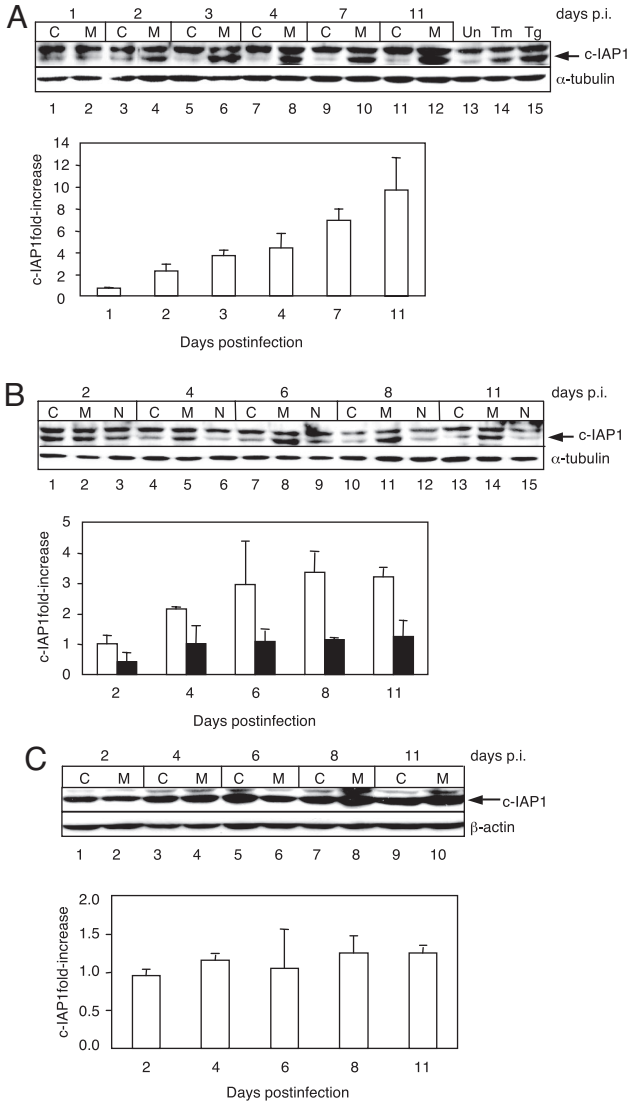

Fig. 3. c-IAP1 protein up-regulation in MCF13 MLV-infected mink cells. Immunoblots of c-IAP1 in mink epithelial cells either mock-infected as control (C) or infected with MCF13 MLV (M) or NZB-9 MLV (N). (*A*) MCF13 MLV infection at a MOI of 20. Mink cells either untreated (Un, lane 13) or treated with tunicamycin (Tm, lane 14) or thapsigargin (Tg, lane 15). (*B*) MCF13 or NZB-9 MLV infection at a MOI of 1. (*C*) c-IAP1 in *M. dunni* fibroblasts either mock-infected (C) or infected with MCF13 MLV (M) at a MOI of 1. Histograms below each immunoblot show the ratio of intensity of the c-IAP1 protein band for virus-infected cells vs. that of the respective control cells as fold-increase. Bars represent cells infected with either MCF13 MLV (unshaded) or NZB-9 MLV (shaded). Cellular protein was analyzed at different days p.i. α-Tubulin or β-actin was detected as a loading control.

Up-Regulation of c-IAP1 Occurs at the Translational Level. We next examined whether the increase in c-IAP1 protein in MCF13 MLV-infected cells was caused by a difference in protein turnover. To determine this, we compared the half-life of c-IAP1 in mock- and virus-infected cells by performing pulse–chase assays. Mock- and virus-infected mink cells at day 5 p.i., when c-IAP1 was up-regulated between ≈4- and 7-fold at a MOI of 20, were exposed to a 30-min pulse of 500 μCi [^{35}S]methionine-cysteine (Met-Cys), after which time cellular extracts were prepared at 0, 6, 16, 24, and 40 h. c-IAP1 was subsequently immunoprecipitated and analyzed by SDS/PAGE. The results for mock- and virus-infected cells from a representative experiment are shown in Fig. 4 *B* and *C*, respectively. From the results obtained from four independent experiments, we calculated mean values and standard deviations for c-IAP1 half-life that were 12.2 ± 1.3 h for mock-infected cells and 12.9 ± 1.1 h for MCF13 MLV-infected cells. Our data thus indicate that there is no effect on the turnover of c-IAP1 because of MCF13 MLV infection. These results suggest that the up-regulation of c-IAP1 depends on translational control.

We further questioned whether an overall increase in total protein synthesis was responsible for the up-regulation of c-IAP1 at the translational level in virus-infected cells. To test this possibility, mock- and MCF13 MLV-infected mink cells at day 5 p.i. were metabolically labeled with [^{35}S]Met-Cys for 30 min, after which time cellular protein was extracted. Ten micrograms of cellular protein was electrophoresed through a 4–20% polyacrylamide gradient gel, which was subsequently transferred to a PVDF membrane and exposed to x-ray film (Fig. 4*D*). The same membrane was subjected to immunoblotting to detect α-tubulin as a loading control. No detectable difference in the overall amount of labeled cellular protein was detectable between mock- and virus-infected mink cells. Because general protein synthesis can be inhibited by high levels of phosphorylated eIF2α (14, 15), our results suggest that either the level of increase in eIF2α-P that is induced by virus infection is not sufficient for inhibition of overall protein synthesis in this cell type, similar to what has been observed for some human cells (21) or the virus uses a mechanism to prevent the inhibition of cap-dependent translation by eIF2α-P. Nevertheless, our data indicate that the up-regulation of c-IAP1 protein is not the result of an increase in global protein synthesis by MCF13 MLV infection, but rather results from specific targeting of its translation. A prominent protein band migrating at ≈80 kDa that was detectable in virus-infected cells most likely corresponds to the precursor polyprotein of the MCF13 MLV glycoprotein (gPr80^{env}) (Fig. 4*D*, lane 2).

Posttranscriptional Up-Regulation in Virus-Infected Cells That Have Survived Apoptosis. Continual passage of mink cells that are acutely infected with MCF13 MLV eventually gives rise to cells that are chronically infected and no longer undergo apoptosis. To determine whether elevated c-IAP1 protein levels persist in these cells, we performed immunoblotting of cellular extracts from uninfected and chronically infected cells. We observed that the level of c-IAP1 protein was ≈4-fold greater in chronically infected cells than in uninfected cells (Fig. 5*A*). To determine whether c-IAP1 up-regulation may be important for tumorigenesis, we examined the level of c-IAP1 protein in thymic lymphomas that were induced by MCF13 MLV inoculation into neonatal AKR/J mice. Thymic lymphomas appeared in animals ≈10–13 weeks after virus inoculation. By immunoblotting, we compared c-IAP1 protein levels in an age-matched control thymus with four different thymic lymphomas (T1–T4) that were excised from moribund animals (Fig. 5*B*). Our analysis revealed 10- to 20-fold higher c-IAP1 protein levels in the thymic tumors compared with control thymus.

To determine whether the up-regulation of c-IAP1 protein in these cells also occurred at a posttranscriptional step, we compared c-IAP1 mRNA levels by qRT-PCR between uninfected and chronically infected mink cells and between control thymus and thymic tumors. Comparison of c-IAP1 transcript levels between the same cells that were used for protein analysis revealed no significantly higher levels in the chronically infected mink cells or virus-induced lymphomas compared with control cells (Fig. 5 *C* and *D*). These results thus indicate that the up-regulation of c-IAP1 protein that was detectable in chronically infected mink cells and thymic lymphomas occurs at a posttranscriptional step, similar to what we have observed for acutely infected mink cells.

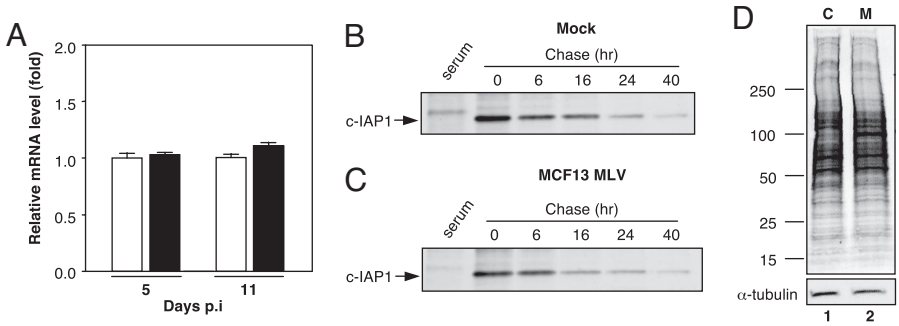

Fig. 4. c-IAP1 up-regulation occurs at the translational level. (*A*) Real-time qRT-PCR analysis of c-IAP1 mRNA in mink epithelial cells either mock-infected (open bar) or MCF13 MLV-infected (shaded bar) at days 5 and 11 p.i. Mean values and standard errors of the mean were calculated from assays of duplicate or triplicate samples from each of two independent experiments (n = 4–6). Results are expressed relative to the level of c-IAP1 mRNA in control cells. (*B* and *C*) Immunoprecipitated c-IAP1 after a 30-min pulse with [^{35}S]Met-Cys and chase for various times from a representative experiment for mock-infected (*B*) or MCF13 MLV-infected (*C*) cells. Serum lane is immunoprecipitation control with normal rabbit serum. (*D*) ^{35}S-labeled protein extracts prepared from mock-infected (C) or MCF13 MLV-infected (M) mink cells were subjected to SDS/PAGE. α-Tubulin was detected by ECL as a loading control. Migration of marker proteins with known molecular masses (kDa) is shown at left.

Discussion

Our results provide evidence for the ability of a simple retrovirus to regulate a cellular gene at the translational level. Whether additional proteins besides c-IAP1 are up-regulated by this mechanism as a result of MCF13 MLV infection remains to be determined. Our detection of a strong correlation between up-regulated levels of eIF2α-P and c-IAP1 in virus-infected mink cells suggests that c-IAP1 translation may involve IRES activity. This hypothesis is supported by studies that have shown that IRES-dependent translation of various cellular mRNAs requires increased levels of eIF2α-P (15–17). The demonstration, moreover, that translation of c-IAP1 mRNA occurs via IRES sequences in the 5′ UTR in cells undergoing ER stress induced by chemical reagents supports this idea (19, 20). Our previous studies have demonstrated that ER stress is also induced as a result of the accumulation of high levels of the MCF13 MLV Env precursor polyprotein in both mink epithelial cells *in vitro* and preleukemic thymic lymphocytes and frank lymphomas isolated from virus-inoculated mice (10, 12). It is thus possible that c-IAP1 up-regulation is occurring via IRES-dependent translation in these cell types. However, other mechanisms for translational regulation that have been identified for mRNAs with long 5′ UTR regions, such as leaky scanning, ribosome reinitiation, and shunting, could also explain our observations for c-IAP1 (18, 22, 23).

Although c-IAP1 and XIAP belong to the same family of antiapoptotic proteins and can be translationally regulated by IRES sequences in their mRNAs, it is interesting to note that XIAP is not up-regulated in MCF13 MLV-infected cells (data not shown). A similar result has been reported for human cells that were treated with tunicamycin and thapsigargin to induce ER stress (20). The differential usage of IRES sequences in the 5′ UTR of cellular mRNAs can be explained by the involvement of specific cellular factors, which may also be cell type-specific, in addition to general ones for their activation (24–27).

The polysomal association of IRES-containing mRNAs appears to depend on specific rRNA interactions that differ from those that affect cap-dependent mRNAs. In a study by Yoon *et al.* (28), it was observed that in cells with a mutation in dyskerin, a protein that acts as a pseudouridine synthase to mediate posttranscriptional modification of rRNA, the association of IRES-containing mRNAs with polysomes was reduced without affecting mRNAs that are translated in a cap-dependent manner. The apparent difference in how IRES-containing mRNAs are associated with polysomes may be another possible explanation for why we have detected c-IAP1 up-regulation in virus-infected cells even though there was no detectable effect on overall cap-dependent protein synthesis (Fig. 4*D*).

The selective up-regulation of a cellular protein is unusual for viruses that manipulate host cell translation because this effect usually results in the overall inhibition of cellular proteins. However, the mechanism that we have described for c-IAP1 synthesis may be relevant to the ability of other cytopathic retroviruses, such as the human and feline immunodeficiency viruses, and neurotropic FrCasE and ts-1 Moloney MLVs, to generate different types of disease, which include immunodeficiency and neurodegeneration (29–32). It is notable that the neurodegenerative MLVs also induce ER stress as a result of retention of the Env precursor polyprotein in the ER (33, 34). For these retroviruses, genetic studies have demonstrated that the Env protein is an important determinant of pathogenicity (35–38). We hypothesize that besides receptor recognition and

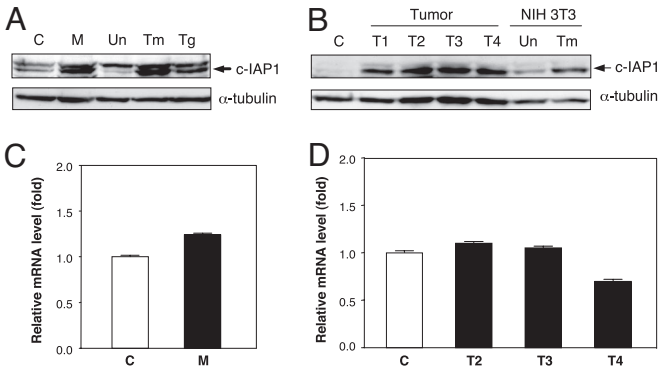

Fig. 5. Elevation of c-IAP1 in mink cells chronically infected with MCF13 MLV and in virus-induced thymic lymphomas at the posttranscriptional level. (*A* and *B*) Detection of c-IAP1 protein by immunoblotting for mink cells either uninfected as control (C) or chronically infected with MCF13 MLV (M) and mink cells either untreated (Un) or treated with tunicamycin (Tm) or thapsigargin (Tg) at 1 μg per ml for 18 h (*A*) and control thymus (C), thymic tumors (T1-T4), or NIH 3T3 fibroblasts that were either untreated (Un) or treated with tunicamycin (Tm) (*B*). α-Tubulin was detected as a loading control. (*C* and *D*) Real-time qRT-PCR analysis of c-IAP1 mRNA in uninfected (C) and chronically infected (M) mink cells shown in *A* (*C*) and control thymus and thymic tumors T2-T4 shown in *B* (*D*). Mean values calculated from triplicate assays and their ranges are indicated for each cell type. *P* values that were determined by Student's *t* test are 0.6 for the comparison between uninfected and chronically infected cells shown in *C* and 0.09–0.8 for comparisons between the control thymus and thymic tumors shown in *D*.

viral entry the Env protein may have an additional role in pathogenesis by affecting host gene regulation at the translational level. It has been observed, furthermore, that translation of retroviral messages can occur via IRES sequences (39, 40). Thus, IRES-dependent translation of retroviral mRNAs in cells undergoing ER stress could potentially result in the augmentation of viral proteins as well.

c-IAP1 (also termed HIAP2, MIHB, and BIRC2) is a member of a family of proteins that inhibit apoptosis, which is achieved by some members by binding different caspases (41). Additionally, c-IAP1 may repress apoptosis via other mechanisms that involve its association with the tumor necrosis factor receptor-associated factor (TRAF) and the ubiquitination of the second mitochondria-derived activator of caspases (Smac/DIABLO) (41). Amplification and overexpression of the c-IAP1 gene in a variety of malignancies, and its cooperativity with the Yap transcription factor to promote tumorigenesis, have led to the proposal that it should be classified as an oncogene (41, 42).

We hypothesize that the up-regulation of the c-IAP1 antiapoptotic protein by translational control contributes to the survival of MCF13 MLV-infected cells from apoptosis, which may be important for tumor development. This idea is supported by our detection of elevated c-IAP1 levels in MCF13 MLV-induced thymic lymphomas and chronically infected mink cells that have survived the cytopathic effects of acute infection. Thus, paradoxically the induction of ER stress by a cytopathic retrovirus can result in either apoptosis or the rescue of a cell from apoptosis. The identity of the factor or factors that regulate this decision by a cell is not known but we propose that cell rescue involves the elevation of a protein or proteins with antiapoptotic activity, which must be at a level above a certain threshold to prevent apoptosis from occurring. It is highly likely that the rescue of cells from apoptosis involves additional proteins with other types of function, such as the regulation of cell cycle and proliferation. The mechanism we have described here may also be important for the development of human neoplasias for which apoptosis occurs as an early event, such as hepatocellular carcinoma (43, 44). Our results underscore the importance of assessing protein levels as well as genetic mutations and transcriptional activity to identify cellular proteins that may contribute to tumorigenesis.

Materials and Methods

Cell Lines, Virus Strains, and Virus Infection Assays. Mink lung epithelial cells obtained from the American Type Culture Collection (CCL64) and *M. dunni* tail fibroblasts were maintained in DMEM supplemented with 10% heat-inactivated FBS (Atlanta Biologicals) and 1% penicillin-streptomycin. Medium for mink cells was also supplemented with 2 mM L-glutamine and 1 mM sodium pyruvate. Cells were mycoplasma-free as determined by routine assays. MCF13 and NZB-9 MLV stocks were prepared from supernatant collected from productively infected *M. dunni* or mink epithelial cells, respectively. Virus titers on each cell type were determined by an indirect immunofluorescence focus assay as described (5).

A total of 10^5 mink epithelial or *M. dunni* cells were plated onto a 10-cm plastic plate. Cells were infected with MCF13 or NZB-9 MLV at a MOI of 1 or 20 in the presence of 5 μg per ml of polybrene. Mock-infected cells were incubated with DMEM and polybrene. After incubation for 6 h at 37°C, viral supernatant was removed, cells were rinsed once with PBS, and fresh medium was added. Cells were passaged every other day after infection.

Immunoblotting and Antibodies. Total cellular protein was prepared as described (45). Protein concentrations were determined by the bicinchoninic acid protein assay (Pierce Biochemicals). Twenty-five to 45 μg of soluble protein was resolved by electrophoresis through a 8% or 10% SDS-polyacrylamide gel and transferred to a PVDF membrane (Bio-Rad). Membranes were incubated with the appropriate primary antibody and horseradish peroxidase-conjugated secondary antibody. Protein bands were visualized with the ECL detection system. c-IAP1 protein was induced by treatment with either tunicamycin or thapsigargin at 1 μg per ml for 18 h. Source of primary antibodies was as follows: anti-eIF2α-P that specifically recognizes phosphorylation at Ser-51 (ab4837) and anti-total eIF2α (ab5369) (Abcam), anti-c-IAP1 (sc-7943), anti-CHOP/GADD153 (sc-793) and anti-GRP78/BiP (sc-13968) (Santa Cruz Biotechnology); anti-GRP78 for the murine protein (SPA-826; Stressgen Biotechnology); anti-α-tubulin (T9026) and anti-β-actin (A5441) (Sigma-Aldrich). Protein bands were quantified by densitometric scanning with a Kodak EDAS 120 scanner and software.

Cellular RNA Extraction and Real-Time qRT-PCR Assays. Total cellular RNA was extracted from 5–7 $\times$ 10^6 cells with the RNAqueous Kit (Ambion). RNA samples were further treated with RNase-free DNase I (RQI; Promega Life Science). RNA preparations were assessed for residual cellular DNA by standard PCRs using primers targeting the c-IAP1 gene. cDNA was prepared for qRT-PCR analysis by using the Mo-MLV reverse transcriptase enzyme (Invitrogen) and random hexamers as primers. SYBR-green-base qRT-PCR was used to assess relative c-IAP1 mRNA levels. Oligonucleotide primers used were as follows: for c-IAP1, 5′ primer, 5′-GCTTGCAAGTGCTGGATT-3′ and 3′ primer, 5′-CAAGAAGATGAGGATATCTAGCT-3′ to yield a 203-bp product; for 18S rRNA, 5′ primer, 5′-CGGCTACCACATCCAAGGAA-3′ and 3′ primer, 5′-GCTGGAATTACCGCGGCT-3′ to yield a 187-bp product. Each sample was run in duplicate or triplicate. Signals from each sample were normalized to values obtained for the 18S rRNA gene, which was assayed simultaneously with the experimental samples. Analyses were performed with a sequence detector (model 7700; Applied Biosystems), and data were analyzed by using the sequence detection software (V.1.9; Applied Biosystems).

Metabolic Cell Labeling, Immunoprecipitation, and PAGE. A total of 10^5 mink epithelial cells were either mock-infected or infected with MCF13 MLV at a MOI of 20 as described above. At day 5 p.i., cells were preincubated in methionine- and cysteine-free medium (Invitrogen) at 37°C for 15 min before the addition of 500 μCi [^{35}S]methionine-cysteine (Perkin-Elmer Life and Analytical Science). After labeling for 30 min, cells were rinsed and resuspended in medium containing 4.8 mM methionine and 7.2 mM cysteine. At 0, 6, 16, 24, and 40 h after pulse labeling, cells were diluted into 10 ml of ice-cold complete medium and rinsed twice with ice-cold PBS. Whole-cell extracts were prepared and protein determinations were made as described above. Immunoprecipitations were performed by preclearing 300 μg of protein with 80 μl of protein A-Sepharose (GE Healthcare Bio-Science) for 1 h at 4°C with rotation. Anti-c-IAP1 polyclonal Ab (H-83) (Santa Cruz Biotechnology) was incubated with precleared protein overnight at 4°C. Normal rabbit serum (Santa Cruz Biotechnology) was used for an immunoprecipitation control. The antibody and protein mixture was transferred to 80 μl of fresh protein A-Sepharose and incubated for 3 h at 4°C. Protein A-Sepharose beads were pelleted and rinsed with wash buffer [50 mM Tris·HCl (pH 7.4), 300 mM NaCl, 5 mM EDTA, 0.1% Triton X-100]. Immunocomplexes were removed by the addition of 2$\times$ loading buffer [62.5 mM Tris·HCl (pH 6.8), 25% glycerol, 2% SDS, 5% β-mercaptoethanol, and 0.01% bromophenol blue dye] to the pellet, followed by boiling for 10 min. Eluates from protein A-Sepharose beads were electrophoresed through 8% SDS-polyacrylamide gels. After electrophoresis, gels were fixed in isopropanol/water/acetic acid (25:65:10), followed by treatment with Amplify Fluorographic Reagent (Amersham Biosciences). Fixed gels were dried under vacuum at 60–80°C for 2 h and exposed to Fuji x-ray film at −80°C for various lengths of time.

Analysis of total cellular protein synthesis was performed by electrophoresis of 10 μg of ^{35}S-labeled protein through a 4–20% polyacrylamide gradient gel (Bio-Rad) at 120 V for 1 h. Protein was subsequently transferred to a PVDF membrane, which was exposed to x-ray film. For loading control, α-tubulin was detected by immunoblotting as described above.

c-IAP1 Half-Life Determination. Half-life calculations were made from densitometric scans of the fluorographs with a Kodak EDAS 120 scanner and software. The logarithmic percentage of remaining band intensity compared with 0-time was plotted against chase time, and half-life values were derived from the equation $t_{1/2} = 0.693/k$, where $k = -2.3m$, and m is the slope of the line obtained by regression analysis. $t_{1/2}$ values correspond to the mean and standard deviations of values calculated from four independent experiments.

Virus Induction of Thymic Lymphoma in Mice. Neonatal AKR/J mice were inoculated i.p. with 50 μl of inoculum containing either 1 to 2.5 $\times$ 10^6 infectious units of MCF13 MLV or tissue culture medium for control animals. Necropsy was performed on moribund mice, which were killed by CO_2 inhalation and cervical dislocation. Animals with the diagnosis of thymic lymphoma showed a massive enlargement of the thymus with fusion of thymic lobes. In the majority of leukemic animals, there was also enlargement of liver, spleen, and peripheral lymph nodes.

ACKNOWLEDGMENTS. We thank M. Clemens for helpful discussions and M. Linial, T. R. Reddy, V. Pain, and A. Shields for critical comments on the manuscript. This work was supported by National Institutes of Health Grants CA44166 and AR42541.

1. Jonkers J, Berns A (1996) Retroviral insertional mutagenesis as a strategy to identify cancer genes. *Biochim Biophys Acta* 1287:29–57.
2. Tupper JC, Chen H, Hays EF, Bristol GC, Yoshimura FK (1992) Contributions to transcriptional activity and to viral leukemogenicity made by sequences within and downstream of the MCF13 murine leukemia virus enhancer. *J Virol* 66:7080–7088.
3. Hartley JW, Wolford NK, Old LJ, Rowe WP (1977) A new class of murine leukemia virus associated with development of spontaneous lymphomas. *Proc Natl Acad Sci USA* 74:789–792.
4. Yoshimura FK, Wang T, Yu F, Kim HR, Turner JR (2000) Mink cell focus-forming murine leukemia virus infection induces apoptosis of thymic lymphocytes. *J Virol* 74:8119–8126.
5. Yoshimura FK, Wang T, Nanua S (2001) Mink cell focus-forming murine leukemia virus killing of mink cells involves apoptosis and superinfection. *J Virol* 75: 6007–6015.
6. Weller SK, Joy AE, Temin HM (1980) Correlation between cell killing and massive second-round superinfection by members of some subgroups of avian leukosis virus. *J Virol* 33:494–506.
7. Rulli K, Lenz J, Levy LS (2002) Disruption of hematopoiesis and thymopoiesis in the early premalignant stages of infection with SL3–3 murine leukemia virus. *J Virol* 76:2363–2374.
8. Brojatsch J, Naughton J, Rolls MM, Zingler K, Young JA (1996) CAR1, a TNFR-related protein, is a cellular receptor for cytopathic avian leukosis-sarcoma viruses and mediates apoptosis. *Cell* 87:845–855.
9. Bonzon C, Fan H (1999) Moloney murine leukemia virus-induced preleukemic thymic atrophy and enhanced thymocyte apoptosis correlate with disease pathogenicity. *J Virol* 73:2434–2441.
10. Nanua S, Yoshimura FK (2004) Mink epithelial cell killing by pathogenic murine leukemia viruses involves endoplasmic reticulum stress. *J Virol* 78:12071–12074.
11. Rutkowski DT, Kaufman RJ (2004) A trip to the ER: Coping with stress. *Trends Cell Biol* 14: 20–28.
12. Yoshimura FK, Luo X (2007) Induction of endoplasmic reticulum stress in thymic lymphocytes by the envelope precursor polyprotein of a murine leukemia virus during the preleukemic period. *J Virol* 81:4374–4377.
13. Harding HP, Zhang Y, Ron D (1999) Protein translation and folding are coupled by an endoplasmic-reticulum-resident kinase. *Nature* 397:271–274.
14. Clemens MJ (2001) Initiation factor eIF2α phosphorylation in stress responses and apoptosis. *Prog Mol Subcell Biol* 27:57–89.
15. Holcik M, Sonenberg N (2005) Translational control in stress and apoptosis. *Nat Rev Mol Cell Biol* 6:318–327.
16. Fernandez J, *et al.* (2002) Regulation of internal ribosome entry site-mediated translation by eukaryotic initiation factor-2α phosphorylation and translation of a small upstream open reading frame. *J Biol Chem* 277:2050–2058.
17. Gerlitz G, Jagus R, Elroy-Stein O (2002) Phosphorylation of initiation factor-2α is required for activation of internal translation initiation during cell differentiation. *Eur J Biochem* 269:2810–2819.
18. Hellen CU, Sarnow P (2001) Internal ribosome entry sites in eukaryotic mRNA molecules. *Genes Dev* 15:1593–1612.
19. Van Eden ME, Byrd MP, Sherrill KW, Lloyd RE (2004) Translation of cellular inhibitor of apoptosis protein 1 (c-IAP1) mRNA is IRES mediated and regulated during cell stress. *RNA* 10:469–481.
20. Warnakulasuriyarachchi D, Cerquozzi S, Cheung HH, Holcik M (2004) Translational induction of the inhibitor of apoptosis protein HIAP2 during endoplasmic reticulum stress attenuates cell death and is mediated via an inducible internal ribosome entry site element. *J Biol Chem* 279:17148–17157.
21. Kim SH, Forman AP, Mathews MB, Gunnery S (2000) Human breast cancer cells contain elevated levels and activity of the protein kinase, PKR. *Oncogene* 19:3086–3094.
22. Sherrill KW, Lloyd RE (2008) Translation of cIAP2 mRNA is mediated exclusively by a stress-modulated ribosome shunt. *Mol Cell Biol* 28:2011–2022.
23. Vattem KM, Wek RC (2004) Reinitiation involving upstream ORFs regulates ATF4 mRNA translation in mammalian cells. *Proc Natl Acad Sci USA* 101:11269–11274.
24. Cobbold LC, *et al.* (2007) Identification of internal ribosome entry segment (IRES)-trans-acting factors for the Myc family of IRESs. *Mol Cell Biol* 28: 40–49.
25. Holcik M, Gordon BW, Korneluk RG (2003) The internal ribosome entry site-mediated translation of antiapoptotic protein XIAP is modulated by the heterogeneous nuclear ribonucleoproteins C1 and C2. *Mol Cell Biol* 23:280–288.
26. Spriggs KA, Bushell M, Mitchell SA, Willis AE (2005) Internal ribosome entry segment-mediated translation during apoptosis: The role of IRES-trans-acting factors. *Cell Death Differ* 12:585–591.
27. Stoneley M, *et al.* (2000) Analysis of the c-myc IRES: A potential role for cell-type specific trans-acting factors and the nuclear compartment. *Nucleic Acids Res* 28:687–694.
28. Yoon A, *et al.* (2006) Impaired control of IRES-mediated translation in X-linked dyskeratosis congenita. *Science* 312:902–906.
29. Shikova E, Lin YC, Saha K, Brooks BR, Wong PK (1993) Correlation of specific virus-astrocyte interactions and cytopathic effects induced by ts1, a neurovirulent mutant of Moloney murine leukemia virus. *J Virol* 67:1137–1147.
30. Meyaard L, *et al.* (1992) Programmed death of T cells in HIV-1 infection. *Science* 257:217–219.
31. Donahue PR, *et al.* (1991) Viral genetic determinants of T cellkilling and immunodeficiency disease induction by the feline leukemia virus FeLV-FAIDS. *J Virol* 65:4461–4469.
32. Clase AC, *et al.* (2006) Oligodendrocytes are a major target of the toxicity of spongiogenic murine retroviruses. *Am J Pathol* 169:1026–1038.
33. Dimcheff DE, Askovic S, Baker AH, Johnson-Fowler C, Portis JL (2003) Endoplasmic reticulum stress is a determinant of retrovirus-induced spongiform neurodegeneration. *J Virol* 77:12617–12629.
34. Liu N, *et al.* (2004) Possible involvement of both endoplasmic reticulum- and mitochondria-dependent pathways in MoMuLV-ts1-induced apoptosis in astrocytes. *J Neurovirol* 10:189–198.
35. Czub S, Lynch WP, Czub M, Portis JL (1994) Kinetic analysis of spongiform neurodegenerative disease induced by a highly virulent murine retrovirus. *Lab Invest* 70:711–723.
36. Freed EO, Martin MA (1995) The role of human immunodeficiency virus type 1 envelope glycoproteins in virus infection. *J Biol Chem* 270:23883–23886.
37. Johnston JB, Power C (2002) Feline immunodeficiency virus xenoinfection: The role of chemokine receptors and envelope diversity. *J Virol* 76:3626–3636.
38. Szurek PF, Yuen PH, Ball JK, Wong PK (1990) A Val-25-to-Ile substitution in the envelope precursor polyprotein, gPr80^{env}, is responsible for the temperature sensitivity, inefficient processing of gPr80^{env}, and neurovirulence of *ts*1, a mutant of Moloney murine leukemia virus TB. *J Virol* 64:467–475.
39. Deffaud C, Darlix JL (2000) Characterization of an internal ribosomal entry segment in the 5′ leader of murine leukemia virus env RNA. *J Virol* 74:846–850.
40. Berlioz C, Darlix JL (1995) An internal ribosomal entry mechanism promotes translation of murine leukemia virus gag polyprotein precursors. *J Virol* 69:2214–2222.
41. Liston P, Fong WG, Korneluk RG (2003) The inhibitors of apoptosis: There is more to life than Bcl2. *Oncogene* 22:8568–8580.
42. Zender L, *et al.* (2006) Identification and validation of oncogenes in liver cancer using an integrative oncogenomic approach. *Cell* 125:1253–1267.
43. Bantel H, Schulze-Osthoff K (2003) Apoptosis in hepatitis C virus infection. *Cell Death Differ* 10(Suppl 1):S48–S58.
44. Papakyriakou P, *et al.* (2002) Apoptosis and apoptosis related proteins in chronic viral liver disease. *Apoptosis* 7:133–141.
45. Nanua S, Yoshimura FK (2004) Differential cell killing by lymphomagenic murine leukemia viruses occurs independently of p53 activation and mitochondrial damage. *J Virol* 78:5088–5096.
46. Zhao, X, Yoshimura, FK (2008) Expression of murine leukemia virus envelope protein is sufficient for the induction of apoptosis. *J Virol* 82:2586–2589.